

RESEARCH ARTICLE

A novel soft polycaprolactone-alginate nanofiber plasma-modified with sufficient cell attachment for tissue engineering

Elham Azizifard ¹, Azadeh Asefnejad ^{*1}, Sedigheh Joughehdoust ¹, Hadi Baharifar ¹

¹ Department of Biomedical Engineering, Science and Research Branch, Islamic Azad University, Tehran, Iran

ABSTRACT

ARTICLE INFO

Article History:

Received 2022-05-04

Accepted 2022-08-06

Published 2023-02-15

Keywords:

Sodium alginate,
Polycaprolactone,
Tissue engineering,
Wound,
Light microscopy.

Degradable polymers belonging to the aliphatic polyester family are currently the most attractive group of synthetic polymers. Natural and synthetic materials used in tissue engineering scaffolds should have properties such as proper biocompatibility and biodegradability with controllable degradation and adsorption rate. Synthetic polymers provide the mechanical support required by the system and the tensile strength for cell attachment and growth. Compared to synthetic polymers, natural polymers are more compatible and reduce the likelihood of tissue rejection after transplantation. Among various hydrogels, collagen and alginate are more widely used for tissue engineering applications. In this article, sodium alginate (SA), polyvinyl alcohol (PVA) and polycaprolactone (PCL) were used to produce porous scaffold. For this purpose, different percentages of SA and PVA were prepared for electrospinning technique. The PCL/80PVA/20SA scaffold was evaluated by Fourier-transform infrared spectroscopy (FT-IR), scanning electron microscope (SEM), light microscopy (LM), biodegradability analyses after plasma process. Morphological examination showed the fiber diameter was about 299 nm and tissue inflation and degradation were reported at 92% and 18%, respectively. The contact angle created is equal to 42° and the biocompatibility study for the scaffold showed 93% survival rate. The obtained results showed that PCL/80PVA: 20SA scaffold after plasma can be used in tissue engineering.

How to cite this article

Azizifard E., Asefnejad A., Joughehdoust S., Baharifar H., A novel soft polycaprolactone-alginate nanofiber plasma-modified with sufficient cell attachment for tissue engineering. J. Nanoanalysis., 10(1): 429-448, Winter 2023. 10.22034/jna.2022.1958065.1300

INTRODUCTION

Degradable polymers belonging to the aliphatic polyester family are currently the most attractive group of synthetic polymers in which the polycaprolactone (PCL) is a biocompatible polymer approved by the Food and Drug Administration (FDA)

for use in medical applications [1-4]. However, it is generally considered as a hydrophobic material. PCL also degrades ester bonds under physiological conditions at a much slower rate than other polymers in this family. Therefore, this group of polymers has

*Corresponding Author Email: asefnejad@srbiau.ac.ir



This work is licensed under the Creative Commons Attribution 4.0 International License.

To view a copy of this license, visit <http://creativecommons.org/licenses/by/4.0/>.

many applications due to its biocompatibility, acceptable degradability rate and adaptability, chemical and physical properties. In this study PCL polymer was used due to some of these advantages [4-8]. Hydrogels are insoluble water-absorbing structure that are modified natural or synthetic polymers and are intended for biomedical applications such as drug release and tissue engineering. These polymers contain a wide range of natural materials such as fibrin, collagen, gelatin, hyaluronic acid, alginate, agarose, chitosan, dextran and chondroitin sulfate can be used with a variety of other materials [9-14]. Among the various hydrogels, collagen and alginate are more widely used for tissue engineering approaches. Alginate is a well-known biomaterial and a natural non-immunogenic and biocompatible polysaccharide obtained from brown algae and some bacteria [15-24]. Due to its high biocompatibility, low toxicity, relatively low cost and gelatinization, it is widely used in tissue engineering application. Gold nanoparticles and doxorubicin (the anti-cancer agent: DOX) were used to inhibit the growth and proliferation of ovarian cancer cells, and gold nanopands can also be used as cell imaging agents due to their unique optical properties [25-43]. Yan et al. [44] fabricated polyvinyl alcohol/chitosan (PVA/CS) hybrid nanofibers containing gold nanorods (Au-NRs) using electrospinning method (ELS). The morphology of PVA/CS nanofibers was examined at different ratios of gold nanoparticles. The results showed that the addition of gold nanoparticles would not affect the morphology as well as the diameter of the fibers. In fact, excessive amounts of metal nanoparticles are not effective in forming electrospun fibers because they break down at electrical pressure. The presence of different functional groups (amino, carboxylic and hydroxyl groups) in these polymers allows chemical modification of enzymatic modification as well as coupling with other polymers to produce different products with the desired chemical and mechanical

properties. The average diameter of nanofibers was about 400 nm, but thinner nanofibers were also observed. Kataria et al. [45] produced a composite of hydrophilic PVA and SA nanofibers as a topical antibiotic delivery system. Electrospinning of SA alone is difficult, so the researchers added PVA to SA to produce composite nanofibers and the antibiotic ciprofloxacin was used as a drug. Researchers have reported their research on the production of electrospun nanofiber scaffolds for dressing applications [46-51]. Three types of polyvinyl alcohol (PVA), polyvinyl alcohol-chitosan (PVA/CS) and polyvinyl alcohol-chitosan-tetracycline hydrochloride (PVA/CS/TCH) scaffolds were produced by ELS method and further morphological, thermal, mechanical, pharmacological, antibacterial properties and cytotoxicity of these scaffolds have been investigated for use in wound dressings. The results showed that although tetracycline was not evenly distributed throughout the nanofibers in the drug-containing sample compared to the drug-free sample. There was little change in morphology and thermal properties and consecutive release of TCH in the first 2 hours provides the right conditions for antibacterial activity against *Escherichia coli* gram-negative bacteria as well as gram-positive bacteria *Staphylococcus epidermidis* and *Staphylococcus aureus*. The results of the MTT test in the laboratory also showed that the nanofiber scaffolds loaded with the drug have good biocompatibility, so the scaffold can be used as an antibacterial wound dressing to heal the wound.

EXPERIMENTAL

Materials and methods

Materials preparation

The specifications of materials and equipment used in the article can be seen in Tables 1 and 2, respectively. Since, sodium alginate cannot be electrospun on its own; an auxiliary polymer like polyvinyl alcohol (PVA) was used. In order to

determine the optimal concentration of polyvinyl alcohol/sodium alginate (PVA/SA) composite scaffolds, three different ratios of 80:20, 70:30 and 60:40 were considered, respectively. The concentration was about 8% for PVA and 4% for SA. The PVA was prepared using distilled water and the resulting solutions were stirred for 8 hours at room temperature with a magnetic stirrer to obtain uniform and clear solutions. On the other hand, sodium alginate solution was prepared with the desired concentration and deionized water solvent at room temperature. PCL solution with a concentration of 12% of chloroform and DMF solvents was used to make a two-nozzle scaffold for another nozzle. In order to prevent solvent evaporation and change the concentration of the solution, the lids of the containers containing the polymer solution are covered with parafilm. Table 3

shows the coding of the solutions and it should be noted that after selecting the sample, the optimal ELS composite scaffold was performed in the form of two dies using PCL. Figure 1 shows the solution was transferred into a 5 cc syringe with a needle with an inner diameter of 0.6. Then insert the syringe into the device and by adjusting the parameters, the ELS process starts and the aluminum foil is placed in front of the needle as a collector. In order to make the nanofibers with high uniform and to create the desired surface, the rotation of the collector plate and the reciprocating movement system of the feed pump were used. Also, all stages of the ELS process have been performed at ambient temperature with the 30% humidity and the ELS conditions for the prepared scaffolds were shown in Table 3.

Table 1. Specifications of materials used in experiments

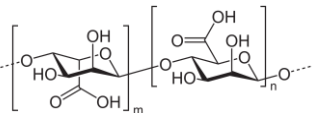
Name of the material	Description	Company Name
PCL	Molecular weight 80,000 daltons	Sigma-Aldrich
PVA	C ₂ H ₄ O	Merck
Sodium alginate salt		Sigma-Aldrich
chloroform	CHCl ₃	Sigma-Aldrich
Dimethylformamide	Mw = 73.09	Sigma-Aldrich
Deionized water	---	Clear-Iran
Phosphate buffer saline solution	PH=7.3 ± (0.1)	DNAbiotech

Table 2. Equipment used in this article

Device name	Device branding	Device model
Digital scales	Japan, FX300I	AND
Stirrer / Hotplate	China, Alfa	H5-860
Electrospinning	Nanoscale-Iran	N1000
Infrared spectroscopy	BOMEM	SRG 1100G
Scanning Electron Microscope	Serontechnologies	AIS2100
Optical microscope	Bell / Italy	MP-bell
Laboratory hood	Service equipment	---
Contact angle	---	CAG-20
Plasma device	Germany- diener	LFG 40

Table 3. Coding and amount of materials used in scaffolding

PCL	SA	PVA	Sample
	4 gr SA in 100 cc DW	8 gr PVA in 100 cc DW	80 PVA : 20SA 1
		80 cc PVA + 20 cc SA	
12 gr PCL in 100 CC Ch:DMF (3:1)	4 gr SA in 100 cc DW	8 gr PVA in 100 cc DW	70PVA : 30SA 2
		70 cc PVA + 30 cc SA	
	4 gr SA in 100 cc DW	8 gr PVA in 100 cc DW	60PVA : 40SA 3
		60 cc PVA + 40 cc SA	



Figure 1. The solution required to make the scaffold using the plasma method

Plasma process on scaffold

In this study, to investigate the effect of plasma on the scaffold the fibers samples were first prepared using ELS device. The scaffold was cut to 8×15 cm and prepared to be irradiated with cold plasma as shown in Figure 1. The plasma process was performed in two stages, each time for 60 seconds, the first stage with a power of 50 watts and a pressure of 0.2 millibars and the second stage with a power of 100 watts and a pressure of 0.2 millibars. The treatment was performed using a cold plasma device of the diener electronic LFG 40 model from Germany available in the Plasma Polymer Research Institute.

Materials characterization

Fourier transform infrared spectroscopy (FT-IR)

This device has the ability to measure the absorption spectrum and the transmission spectrum in the range of 500-cm^{-1} to 4000 cm^{-1} . The qualitative analysis of compounds that have an infrared radiation

absorption band may be easily possible. The test was performed for PCL/80PVA:20SA samples with and without plasma using SRG-1100G infrared spectroscopy device.

Morphological study

A light microscope was used for the initial observation of the porous scaffolds and the absence of spot in the nanofibers. The light microscope used is DM4- model which was performed for 80PVA 20SA, 70PVA:30SA, 60PVA:40SA and PCL samples. Scanning Electron Microscope (SEM) was used to evaluate the scaffold surface. First, the samples were coated with gold and then imaging was performed and the size of fibers and porosity were measured by Image-J software. The SEM tool used is AIS2100 model, which was performed for PCL/80PVA:20SA samples with and without plasma and to examine the adhesion of cells on the scaffold.

Evaluation of inflation rate

Water absorption test is used to check the

swelling rate therefore for this purpose, first the weighed samples (dry weight), after immersion in phosphate buffer saline (PBS) for 5 seconds, their weight (fresh weight) is measured again and from Equation 1. Then, the amount of absorption can be obtained.

$$\text{Water Absorption (\%)} = [(W-W_0)/W_0] \times 100 \quad (\text{Eq. 1})$$

Where W_0 is the dry weight and W is the weight of the immersed scaffold. Water absorption test was performed for PCL/80PVA:20SA samples with and without plasma.

Biodegradability

In order to evaluate the stability and measure the degradation rate in the external environment, hydrolytic biodegradability test was used, so first the scaffold is weighed (dry weight) and placed in PBS for 10 hours and every 1 hour, the samples were measured. The percentage of biodegradability of the compound is obtained from Equation 2.

$$\text{Biodegradability (\%)} = [(W-W_1)/W_1] \times 100 \quad (\text{Eq. 2})$$

Where W is the dry weight and W_1 is the weight of the immersed scaffold. Biodegradability test was performed for PCL/80PVA: 20SA samples with and without plasma.

Measuring the contact angle

The contact angle of the fluid droplet on the solid surface can be measured. The main applications of measuring contact angle are to determine the degree of hydrophobicity or hydrophilicity, self-cleaning, surface energy and other surface properties. Contact angle measurement is done by Drop Sessile Method (DSM). A droplet of a specified size (approximately 4 μ l in ASTM D7334) is placed on the sample surface. The droplet is then photographed with a high-precision camera (CCD camera) and the contact angle of the three-phase line at the point where the droplet meets the surface. The above image is processed and angles are calculated with the support of image processing

software. The size of the samples is 5×5 cm, and 3 drops are placed on each sample. The device used to test the contact angle of the CAG-20 model was performed for PCL/80PVA: 20SA samples with and without plasma.

Cell culture test (In vitro)

This test was performed indirectly in accordance with the requirements of ISO10993-5. To prepare one-day extracts, a sample of 3 cm^2 was prepared and placed in a sterile microtube. Then, 1 ml of RPMI culture medium without fetal bovine serum (FBS) was poured on them and placed in an incubator. In-incubation culture conditions include 5% carbon dioxide, 90% humidity and 37°C. The floor plate of 96 houses (one hexagonal column at a time) was also used as a negative control (no cytotoxic response). Dimethyl thiazole diphenyltetrazolium bromide (MTT) test with a concentration of 0.5 mg/ml was used to evaluate the toxicity. Thus, 5,000 L929 cells per 100 μ l of culture medium (RPMI) containing serum were first poured into three 96-well plate wells for each of the two samples and a column as a control. After first day, the culture medium was removed and 100 μ l of extract containing 10% serum was added to each well and added to the control column of FBS medium. After 24 hours, the extract was removed and 100 μ l of MTT solution was poured into each well. After four hours, the medium was removed from the cells and 100 μ l of isopropanol was added to them and placed in an incubator for 20 minutes to dissolve the purple crystals of Formazan. Then, the amount of adsorption of the solute in isopropanol at 545 nm was calculated with ELISA reader (StatFax 2000). Wells with more cells show higher optical density (OD) than wells with fewer cells. Therefore, it is possible to determine the number of cells with more cells from the sub-well relation and compare it with the control sample.

$$\text{Toxicity\%} = \left(1 - \frac{\text{mean OD of sample}}{\text{mean OD of control}}\right) \times 100 \quad (\text{Eq. 3})$$

$$\text{Viability}\% = 100 - \text{Toxicity}\%$$

(Eq. 4)

The color of MTT in living cell mitochondria changes from yellow to purple formazan crystals and the color concentration is a measure of the number of living cells. The percentage of cell viability is in accordance with the diagrams that can be discussed later and indicates the lack of cell toxicity of the samples. It should be noted that toxicity test was performed for the sample with PCL/80PVA:20SA with and without plasma for the first and third day.

Proliferation of fibroblast cells

In the current study, L929 cell (NCBI-C161) taken from the cell bank of Pasteur Institute of Iran was used. After defrosting the cells, they were transferred to a flask containing DMEM culture medium with 10% FBS and then the flask was incubated at 37°C, 90% humidity and 5% carbon dioxide concentration. It should be noted that the culture medium was changed every 3-4 days. First, the sample was cut in dimensions of 1 × 1 cm and placed in the bottom of the wells of the cultivation plate of 12 houses. The samples were first sterilized with 70% alcohol and then with UV.

Cell adhesion analysis

To check cell adhesion, sterilized samples were placed in each of the plate wells of 12 sterile cells. Then 20,000 cells in a volume of 80 microliters were poured on each sample and incubated for 4-5 hours. After the cells adhered, a certain amount of culture medium including 10% FBS was added to each well. After 24 hours, the culture medium was removed from the samples and washed with PBS for 30 seconds, and then 3.5% glutaraldehyde was used for cell fixation. In this way, after pouring a certain amount of fixative on each of the samples, it was placed in the refrigerator for two hours and then the fixative was removed and the samples were divided into two series with deionized water and alcohols of 50%, 60%, 70%, 80% and 96% was washed. The cell adhesion to the samples was then examined by AIS2100 and SEM.

RESULTS AND DISCUSSION

Tissue engineering structures with desirable biomimetic and mechanical properties were created due to the complexities of conventional skin graft. They facilitate tissue regeneration without compromising mechanical properties. Many researchers have reported the construction of PCL scaffolds by fused deposition modelling (FDM) and immobilizing gold nanoparticles on the polymer surface after modifying the PCL surface using plasma polymerization. The 3D printed PCL scaffolds with gold nanoparticles (Au-PCL) due to their structural and mechanical properties were investigated using FE-SEM tools. Hydrophilicity was determined using water contact angle studies and the surface topography was imaged under atomic force microscopy (AFM). Modifying the surface of 3D printing scaffolds significantly improves their hydrophilicity, indicating that PCL hydrophobicity for biological applications. Nanostructured studies showed that PCL-Au-scaffolds showed a significant increase in mechanical properties by decreasing the elastic modulus of 1.81 GPa. Biocompatibility was assessed by measuring cell viability, cell adhesion and immune response. Biocompatibility *in vitro* studies showed that living cells can be attached to the 3D printing network of gold nanoparticles. The plasma modification and immobilization of gold nanoparticles on PCL scaffold is a simple and cost-effective technique to increase the mechanical properties and biocompatibility of hydrophobic scaffolds such as PCL, thus making it a very promising tool for future scaffold applications. The cold plasma activated water (PAW) was investigated in the preparation of sodium alginate (SA) solution and the effect of reactive oxygen and nitrogen species. The films were evaluated, citric acid (CA) was added to SA, and the combined effect of PAW and CA on the functional properties of SA films was evaluated. By adding 0.5, 1 and 2 wt% of CA, the tensile strength

of the films decreases, while an increase in length is observed. Addition of glycerol reduces tensile strength and tensile modulus [52-64]. Electrospinning technique is also a new processing method for biodegradable polymers, which gives us the ability to produce ultra-thin polymer fibers with diameters ranging from a few micrometers to 10 nanometers. The ELS technique of polymers, in addition to reducing the dimensions of these materials at the nanometer or micrometer level, allows shaping materials that are morphologically similar to extracellular fluid (ECM) of many body tissues and lead to dependence control [65-68].

The stage of structural repair can be divided into the formation of new granulation tissue and changing the position of granulation tissue into a scar which is characterized by the replacement of fibrin mass with fibroblast tissue filled with capillaries. Within two days of injury and after the inflammatory phase is over, fibroblasts begin to migrate from around the skin membrane into the mass, and new capillaries regenerate in the fibroblast tissue. Fibroblast cells are the main cells located in connective tissue and are responsible for the synthesis and secretion of connective tissue compounds and precursor molecules of various types of collagen and elastin fibers. Fibroblasts are spindle-shaped and have all the characteristics of active protein-producing cells. The group that originates in the bone marrow makes both type I and type III collagen, while fibroblasts located at the site of injury make type I collagen. In order to evaluate wound healing, fibroblast cell culture on PCL-alginate mesh may be used. The aim of this study was to investigate the biocompatibility of PCL-alginate nanofiber meshes obtained by electrospinning and the effect of plasma surface modification on the physical properties of scaffold for tissue engineering applications. The surface modification of biomaterials can be done by various techniques such as correction by radiation, charge discharge, plasma, photons,

electron beam, ion beam and X-ray obtained.

In this study, in order to create a structural similarity of the polymer used to the ECM to increase the growth and proliferation of fibroblast cells, this technique is used. It should be noted that repairing a skin injury can be divided into three close integrated stages as prevention of bleeding (coagulation), inflammation and structural repair. In this study, the plasma surface modification process was selected to modify the surface of PCL electrospun meshes. Plasma modification is a widespread and effective method for modifying the surface properties and introducing the desired chemical groups to the surface of a material without affecting the bulk properties of that material. The most noticeable effects of plasma surface modification include surface cleaning, micro-etching, surface activation (by bonding chemical groups) and increasing surface free energy. A common application of this method is to increase the hydrophilicity of the surface by forming oxygen-containing groups on the surface of the material. In recent years, plasma surface modification has been used extensively in biomaterial research. The properties of modified and unmodified PCL-alginate nanofibers may be measured and determined using techniques such as SEM, contact angle measurement and ATR-FT-IR. These techniques make it possible to evaluate changes in surface topography, hydrophilicity, and surface chemistry created by surface modification. Preparation of surface modified PCL-ALG scaffold for use in tissue engineering and regenerative medicine. The MTT test may be performed on biocompatibility on cultured fibroblast cells on a sample of PCL -alginate nanofibers. Figure 2 shows the FT-IR of PCL/80PVA:20SA without plasma. The PCL spectrum showed several characteristic peaks that were associated with asymmetric and symmetric CH₂ tensile vibrations for Figure 2, 1238 and 1165 cm⁻¹, respectively. 1722 cm⁻¹ showed tensile vibration C=O in carbonyl groups. Peaks 2941 and 2866 cm⁻¹ are

related to asymmetric and symmetric tensile vibrations C-O-C, respectively. The main peaks associated with PVA belong to the C-H, OH and C-O groups, which are clearly shown in Figure 2. For example, the broad alkyl tensile bond C-H (2941 cm^{-1}) and the normal strong hydroxyl bond for free alcohols can be seen in the hydrogen bond (3318 cm^{-1}). Intramolecular and intermolecular hydrogen bonds are expected to occur between PVA chains due to strong hydrophilic forces. The peak range of 1165 cm^{-1} corresponds to the C-O (crystallinity) band. This bond is used as a tool to evaluate the structure of PVA because it is a synthetic, semi-synthetic, semi-crystalline polymer that is able to form some domains related to several process parameters. Absorption bands of carboxyl, ether and hydroxyl functional groups appeared well in the spectrum [69-71]. The use of alginate to reduce the hydrophobicity of PCL and to investigate the effect of surface modification on hydrophilicity and biocompatibility of scaffolds are among the innovations of this research. The OH bond tensile bands appeared in the 3318 cm^{-1} range. The band observed in 2941 cm^{-1} was attributed to the tensile band of the aliphatic C-H group. Symmetric carboxylate adsorption bands (COOH) were observed at 1418 cm^{-1} . The plasma process can clean the surface of potential contaminants, improve surface adhesion, increase

surface energy (or wettability), improve biocompatibility, reduce surface friction, descaling the surface, and functionalize the surface. Cold plasma is suitable for surface modification of heat-sensitive materials such as biodegradable polymers. Plasma forms active groups on the surface of the polymer that, upon reaction with oxygen, carboxyl, and hydroxyl groups on the scaffold surface [66-72]. Nanofibers are more sensitive to plasma surface modification due to their higher specific surface area. It should be noted that the characteristics created by the plasma process are not permanent [52]. Figure 2 shows the infrared spectrum of the PCL/80PVA: 20SA scaffold on which the plasma process is performed and the peak is very weak in the range of 2866 cm^{-1} . The peak in the range of 1163 cm^{-1} belongs to the PVA ester tensile group, which has increased sharply after plasma. Peaks 1256 , 1141 and 1056 cm^{-1} belong to the C-O ester tensile group [52]. Methylene peaks 1532 cm^{-1} and 1368 belong to CH_2 and CH_3 groups, respectively. Figure 2 shows a comparison of both spectra obtained to investigate plasma treatment on the scaffold. The image shows that the intensity of the peaks generally increased after the plasma process. On the other hand, new peaks have appeared that show the effects of plasma on the scaffold.

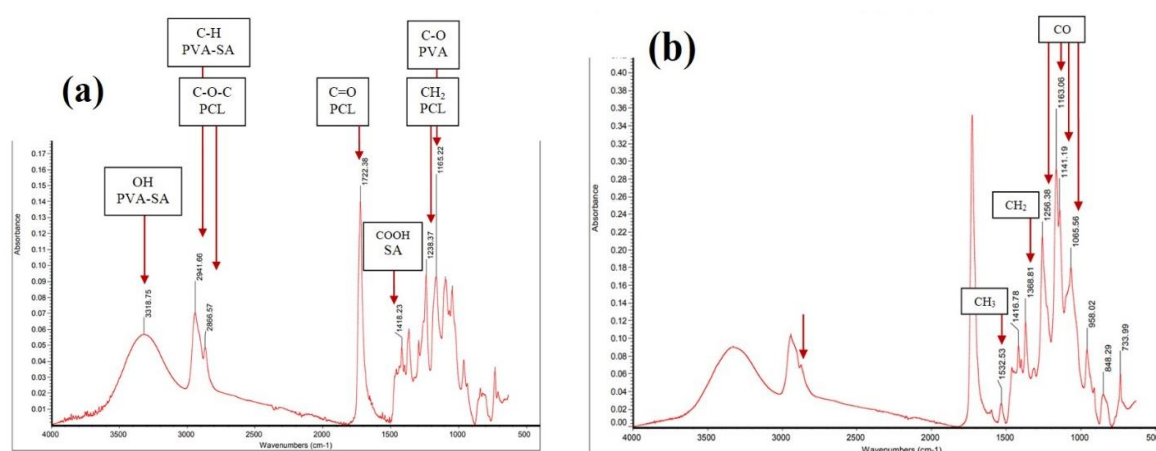


Figure 2. FT-IR analysis of a) PCL/80PVA scaffold infrared spectroscopy: 20SA without plasma and b) PCL/80PVA scaffold infrared spectroscopy: 20SA with plasma

Figure 3 shows a light microscope image of PVA and sodium alginate electrospinning at different percentages without plasma treatment in which Figure 3-a shows for 80PVA: 20SA scaffold and the observation indicated that the fibers are with low porosity. However, with increasing the percentage of alginate, the viscosity of the solution changed and led to the formation of porous fibers. As shown in Figures 3 (b-c) (70PVA: 30SA and 60PVA: 40SA), with the increase of sodium alginate, the formation of moths also increased. Therefore, it was decided to use 80PVA: 20SA scaffold for further studies. Figure 3 (d) is related to PCL scaffold; the fibers have a suitable morphology. Figure 4 shows the morphology of scaffolds before and after plasma treatment using SEM at two different scales. Figure 4-a shows the PCL/80PVA: 20SA scaffold before plasma treatment. The average diameter of 20 selected fibers is 299 nm, which is in the range of 151 to 422 nm. Figure 4-b shows the PCL/80PVA: 20SA scaffold after plasma treatment. The plasma process has affected the morphology of the scaffold, causing a flattening of the fibers. Plasma can make changes in the open space between fibers, point joints or fiber melting [53]. The average diameter of fibers is 361.2 nm and in the range of 117 to 575 nm. Figure 5 shows the average diameter of the fibers. The fiber diameter has increased with the plasma process. Figure 6 shows the swelling percentage of PCL/80PVA:20SA scaffold with and without plasma process. The plasma-free scaffold has less swelling than the scaffold after the plasma process. Since, SA and PVA are composed of hydroxyl groups, they have been able to show swelling up to 70.94%. After the process, the water absorption rate has increased to 92.09%. To evaluate the biodegradability of the scaffolds, they were placed in PBS solution for 10 hours and their weight was examined every 1 hour. Figure 7 shows the percentage of degradation in 10 hours for PCL/80PVA scaffold: 20SA with and

without plasma. As shown in the diagram, both scaffolds have been destroyed over time. However, the percentage of degradation for PCL/80PVA: 20SA scaffold with plasma treatment is higher than PCL/80PVA: 20SA scaffold without plasma treatment. Because the hydrophilicity of the scaffold has been increased by modifying the surface, it can absorb more water, which destroys the molecular chains. Figure 7 (a-b) shows the demolition for scaffold without treatment. In the first 1 hour, 2.56% of the scaffold was destroyed. After 5 hours, 9.40% of the destruction occurred. In the first 1 hour 6.97% and during 5 hours 13.95% destruction occurred. In both scaffolds, the destruction rate decreased after 5 hours. The reason for this can be considered as free OH groups for PVA and sodium cross-linked SA [51-54]. During the second 5 hours, the destruction process was slower. The reason for this slow degradation is related to PCL because PCL degradation is very slow. Huang et al. [12] stated that the rate of PCL degradation is related to the percentage of PVA. They made a film of PCL and PVA and stated that after placing the film in water, cracks formed after dissolving on the film because PVA dissolution promotes PCL dissolution. In recent years, significant advances in nanotechnology have taken place in a variety of industries. Among these, nanofibers as one of the most important nanostructures have been highly regarded by scientists. Polymer nanofibers are currently receiving a great deal of attention due to their unique properties such as large surface area, high porosity, small pore size, superior mechanical properties and higher surface usefulness than any other material [22-28]. Polymer nanofibers can be used in various industries for various applications such as filtration, sensors, protective clothing, etc. and in the medical industry as a framework (scaffold) in tissue engineering and controlled drug release [29-34].

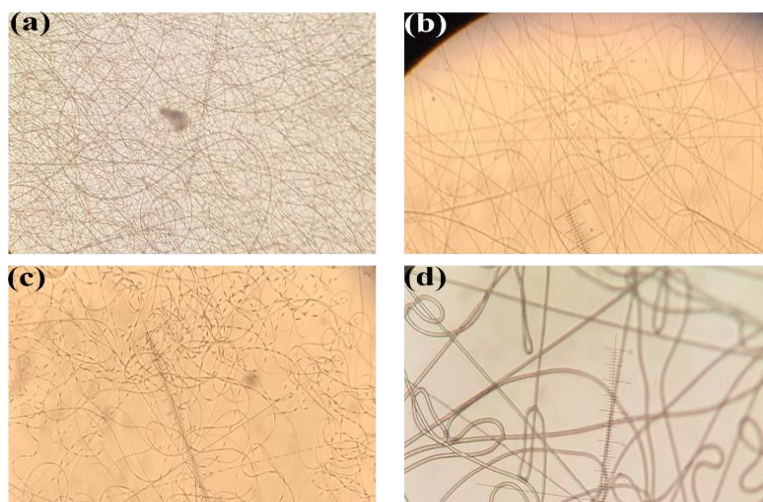


Figure 3. Optical microscope. a) 80PVA scaffold: 20SA, b) 70PVA scaffold: 30SA, c) 60PVA scaffold 40SA and d) PCL scaffold

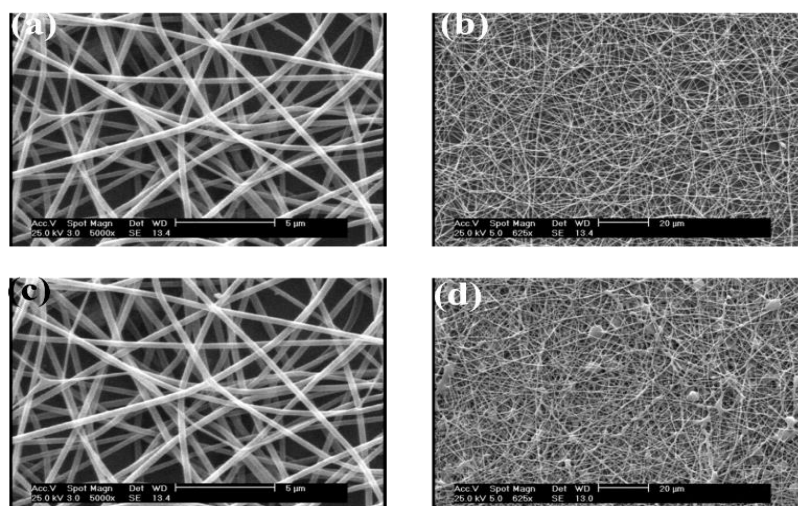


Figure 4. SEM microscope PCL/80PVA scaffold: 20SA, a-b) without plasma treatment, c-d) with plasma treatment

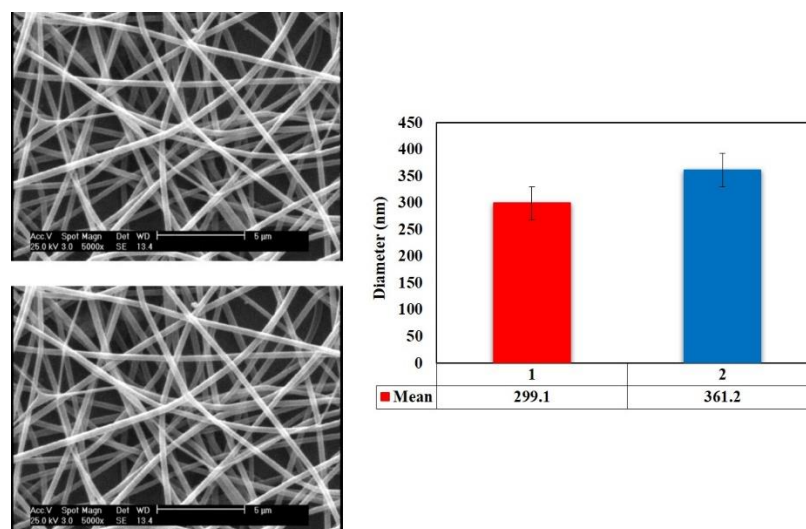


Figure 5. Diagram of average diameter of PCL/80PVA scaffold fibers: 20SA, a) without plasma treatment, b) with plasma treatment

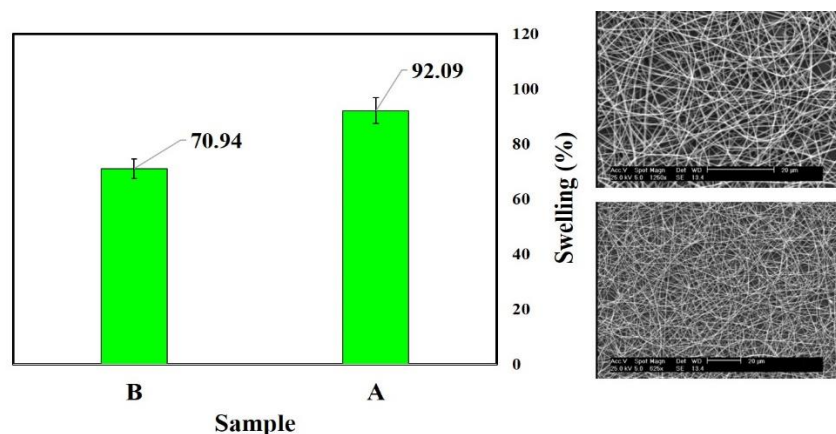


Figure 6. PCL/80PVA scaffold swelling percentage chart: 20SA after 5 seconds, with plasma treatment, and without plasma treatment

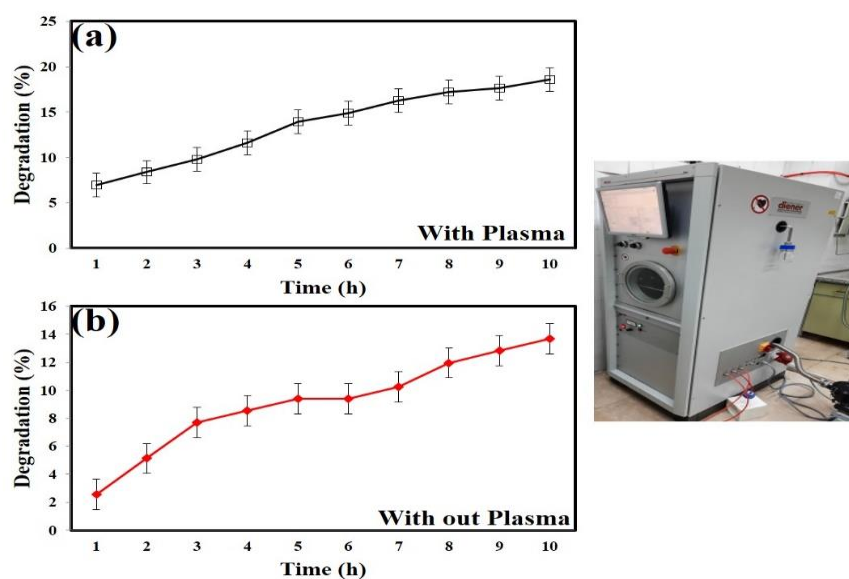


Figure 7. PCL/80PVA scaffold degradation process: 20SA, blue curve: no plasma, red curve: with plasma

Polymeric nanofibers prepared by the ELS process can be used as a scaffold for the delivery and release of selected drugs such as bioactive molecules (cytokines), growth factors, anticancer drugs, enzymes and wound healing, and certain vitamins.

The major advantages of nanofiber scaffold structure in drug delivery applications include excellent stability, better targeting, minimal toxicity, high drug loading capacity, exceptional mechanical properties, encapsulation of different amounts of drug, and suitability for heat-resistant drugs. One of the most popular techniques for the production of nanofibers is electrospinning, which is used to make various types of nanofiber scaffolding. The ELS method is the process

of converting a polymer solution/melt (or without additive) into nanofibers using electrical force. Among the common methods reported for the production of nanofibers such as design, mold synthesis, phase separation and electrospinning, electrospinning due to its advantages such as easy control of fiber diameter, morphology, surface properties, automatic production, fiber pulling, porosity and ease in obtaining fiber diameter is more popular in the nano range [25-39]. Recently, repairing damaged tissue is one of the most important concerns of biologists, so the need for electrospun nanofibers in tissue engineering and reconstructive medicine is felt more than ever. Tissue engineering allows us to produce a new tissue with the

support of stem cells or differentiated cells of the same tissue. Creating new tissue outside the body requires a substrate to place cells on it and mimic the extracellular matrix inside the body, which is called a scaffold. In tissue engineering, cells are placed on the scaffold and the set of cells and scaffold is grown with culture medium. Nanofibers mimic ECM. Interaction between cells and ECM can affect cellular activities such as adhesion, migration, proliferation, differentiation and gene expression. Therefore, the better the scaffold can imitate the ECM, the more likely it is to succeed in retrieving and reaching the desired tissue. The electrospun nanofibers act as a scaffold for the cells and remain in the body until the extracellular matrix is restored. Although the desired properties for a nanofiber scaffold vary according to the type of texture, there are a number of common characteristics that are desirable for all textures. Biocompatibility, biodegradability, arrangement, porosity, unevenness and surface hardness of nanofibers are among the characteristics that should be considered in the design of nanofiber scaffolds. To build drug delivery systems based on these methods, the drug is combined with a polymer in an electrospun solution. In this method, the diameter and shape of the fibers are determined by three general variables: environmental parameters (temperature, humidity, and air velocity in the spinning chamber), controlled parameters of the equipment (solution flow velocity, electric field applied and tip to collector distance), and soluble parameters (soluble dielectric constant, conductivity, polymer type and polymer concentration, and surface tension) are determined. Fibers in a sentence are very narrow strands that are longer than their diameter and have different uses. Fibers are generally divided into natural and synthetic. Natural resource constraints have led scientists to turn to synthetic fibers. Fibers usually have a diameter in the range of 5 to 500 micrometers, but in recent years with the development of nanotechnology, the production of fibers with a diameter of nanometers

has received much attention.

Nanofibers are defined as fibers with a diameter of less than 100 nm and have a dimension outside the nanometer range and belong to the category of one-dimensional nanomaterials. Very high surface-to-volume ratio (this ratio is approximately 1000 times that of microfibers in the case of nanofibers), high flexibility in functionalizing surfaces, and excellent mechanical properties such as tensile strength are among the properties of nanofibers compared to conventional fibers. These outstanding properties make nanofibers a good choice for many important applications. Drug release from nanofibers can be due to drug adsorption from the surface, diffusion from the surface and penetration through the pores, or decomposition of the fiber matrix. All of these currents and drug release stages are likely to be influenced by the choice of inactive materials (polymeric materials or other materials), porosity, morphology, and geometry of the nanofibers. In general, the smaller diameter of nanofibers and their faster release and diffusion are considered based on the fact that fibers with smaller diameters have a larger surface area and a higher dissolution percentage. Subsequent findings showed that drug release and release could not be a function of diameter alone, and that the simultaneous effect of porosity should be considered. It is often the case that thicker nanofibers with very high porosity increase the release rate of the drug compared to thinner fibers with less porosity. The regulation of nanofibers is another parameter that is known to affect the release and release of drugs and in general is a random pattern with faster drug release, which is due to the greater tendency to absorb water.

PVA is a water-soluble synthetic polymer in the form of a white, molten powder that decomposes at 230°C and is stable, dry, odorless, informal, and safe to carry by hand. Environment. PVA has a very attractive property and that is its biodegradability. PVA is soluble in hot and cold water and for example, PVA is soluble

in hot and cold water by 88% hydrolysis, but PVA is soluble in hot water only by 98% hydrolysis. Vinyl alcohol monomers are weak and PVA is prepared by replacing the acetate group in vinyl acetate with hydroxyl groups [37]. Li et al. [15] coated the surface of iron nanoparticles with PVA, the results of which showed that increasing the amount of PVA reduced the crystallinity of the particles while their size remained almost constant. Due to the excellent film-forming properties, the amount of PVA added to the iron oxide nanoparticles is very important. The best amount of PVA is 2 to 3 times the weight of iron. Sodium alginate is a polysaccharide that is structurally and chemically similar to the exopolysaccharide produced by these mucosal species. Its use in antibiotic testing has shown a decrease in gentamicin activity, while having no observable effect on neutral or negatively charged beta-lactam antibiotics. The most important property of alginate, which has increased the importance of this polymer for industrial and biotechnological applications, is the ability to create electrostatic bonds between the chains of this polymer with divalent ions such as Ca^{+2} , Sr^{+2} , Ba^{+2} and the formation of hydrogels. Table 4 shows the percentage of degradation within 10 hours for PCL/80PVA:20SA scaffold with and without plasma treatment. After 10 hours, the degradation for

plasma and non-plasma scaffolds is 18.60 and 13.67%, respectively, the result shows that the plasma process has increased the degradation of the scaffold. The hydrophilicity of the fiber networks was determined by measuring the contact angle of the water droplets. Typically, superhydrophilic surfaces create a contact angle between zero and 30° , and surfaces with hydrophilicity show a contact angle of up to 90° .

Table 5 shows the contact angle size for PCL/80PVA scaffold:20SA with and without plasma. The contact angle decreased from 53.23° to 42.86° after the plasma process. This decrease of 10° indicates that the plasma has increased the hydrophilicity of the scaffold. To evaluate the biological properties of scaffolds, their viability and cytotoxicity have been studied. As mentioned in Table 5, the survival rate for PCL/80PVA: 20SA scaffold after plasma treatment on the third day is 93.36%, which is 74.01% for non-plasma treatment scaffold. The cell viability percentage for scaffolds with and without plasma on the first day was 97.15% and 88.61%, respectively. Survival percentage results show that after 3 days, the treated scaffold is more biocompatible. Accordingly, the percentage of toxicity for the same scaffold after three days is equal to 6.64%, while the rate of toxicity for scaffold without treatment is equal to 25.99 percent.

Table 4. Electrospinning conditions for different solutions

Collector speed (rpm)	Feeding rate (ml/h)	Voltage (Kv)	Distance (cm)	Sample
1000	0.5	17	15	80 PVA: 20SA
1000	0.5	17	15	70 PVA: 30SA
1000	0.5	17	15	60 PVA: 40SA
1000	0.5	15	15	PCL

Table 5. Percentage of degradability of PCL / 80PVA scaffold: 20SA

Time	Percentage of scaffold destruction without plasma	Percentage of scaffold degradation with plasma
1 hour	%2.564103	%6.976744
2 hours	%5.128205	%8.372093
3 hours	%7.692308	%9.767442
4 hours	%8.547009	%11.62791
5 hours	%9.401709	%13.95349
6 hours	%9.401709	%14.88372
7 hours	%10.25641	%16.27907
8 hours	%11.96581	%17.2093
9 hours	%12.82051	%17.67442
10 hours	%13.67521	%18.60465

Figure 8 shows a comparison of cell viability for scaffolds with and without plasma for the first and third days. As it turns out, scaffold A (with plasma) has a higher survival rate than scaffold B (without plasma). For more detailed examination, cell adhesion test was performed on the scaffold with and without plasma. Figure 9-a, is a plasma scaffold and Figure 9-b is a plasma-free scaffold. As can be seen in the images, more cell adhesion occurred on scaffold a, than scaffold b because the surface correction of the scaffold caused more adhesion on the scaffold. It can be inferred that the porosity of the scaffold is optimal because the

culture medium has penetrated into the underlying layers of the scaffold. Tissue engineering and replacement of damaged tissues is very important in medical science and is more efficient than organ transplantation from one person to another. Therefore, the preparation of scaffold from natural and synthetic polymers with desirable properties in order to regenerate damaged tissues is increasing. The materials used in the preparation of scaffolds can be natural, artificial or mineral, which must be biocompatible and biodegradable. Another necessary feature to have a suitable scaffold is hydrophilicity.

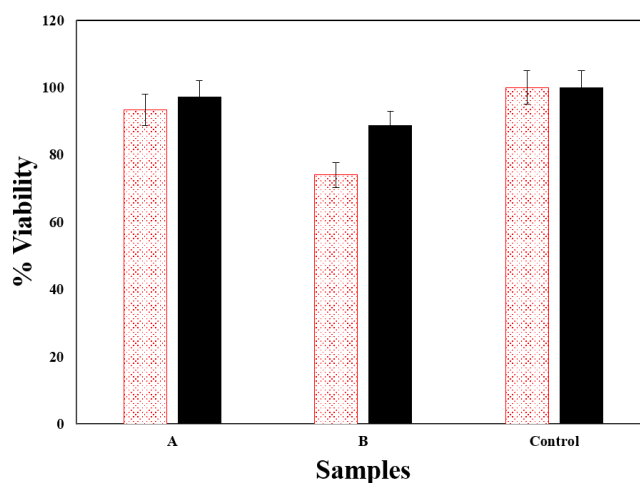


Figure 8. Survey of PCL/80PVA scaffold survival percentage: 20SA, a) first day, b) third day, orange diagram (with plasma, purple diagram) without plasma

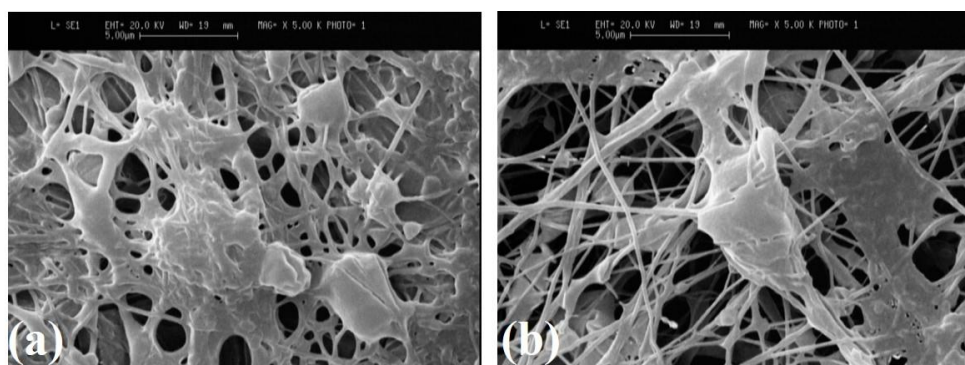


Figure 9. Cell adhesion: a) with plasma treatment, and b) without plasma treatment

CONCLUSION

The hydrophilicity of the surface causes better adhesion and cell growth on the scaffold. Natural polymers such as collagen, chitosan, etc. have good hydrophilicity, but most synthetic polymers do not have the hydrophilicity required for use in tissue engineering. Synthetic PCL polymer has many applications in tissue engineering and has suitable mechanical properties for the culture process. Compared to natural polymers, this polymer does not have the necessary hydrophilicity for cell growth. There are various methods to increase the hydrophilicity of hydrophobic polymers, such as coating with hydrophilic particles, mixing with the surface of hydrophilic non-ionic activities, creating surface roughness, increasing the porosity of the layer, plasma, and so on. In this study, we tried to increase the hydrophilicity and biocompatibility of the scaffold with the plasma process. The study of factor groups using FT-IR test for scaffolds with and without plasma showed differences in the peak. The formation of nodes such as C-O, C = O, CH₂ and CH₃ is an example of plasma treatment. Between concentrations of 20, 30 and 40%, the most suitable concentration for alginate is 20%. Electrospinning of PCL fibers was observed without moth. More detailed morphological studies were performed using a SEM on PCL/80PVA:20SA scaffold, which is a moth-free scaffold with an average fiber diameter of 299 nm. The morphology of the scaffold has changed after plasma treatment; the

junction of the fibers has become a melting state. This has increased the diameter of the fibers to 361 nm. Inflation analysis has shown that the plasma process has increased water absorption from 70.94% to 92.09%. Biodegradability was higher for scaffolds on which the plasma process was performed than for scaffolds without plasma. After 10 days, the scaffold was destroyed with 18.60% plasma. Surface treatment of scaffolds has increased the adhesion on the scaffold. As the scaffold without plasma is 13.67% destroyed. Examination of contact angle on scaffold with plasma showed lower contact angle (42.86°) and scaffold without plasma showed larger angle (53.23°). The evaluation of cell survival percentage after three days on plasma scaffolds was 93.36% and without plasma scaffolds was 74.01%. The results show that PCL/80PVA: 20SA scaffolds improved after plasma treatment process. Therefore, the scaffold can be used in tissue engineering.

ACKNOWLEDGEMENTS

The authors would like to extend their gratitude for the support provided by department of Biomedical Engineering, Science and Research Branch, Islamic Azad University, Tehran, Iran.

REFERENCES

- [1] Khandan, A., Abdellahi, M., Ozada, N., & Ghayour, H. (2016). Study of the bioactivity, wettability and hardness behaviour of the bovine hydroxyapatite-diopside bio-nanocomposite

- coating. *Journal of the Taiwan Institute of Chemical Engineers*, 60, 538-546.
- [2] Karamian, E., Motamedi, M. R. K., Khandan, A., Soltani, P., & Maghsoudi, S. (2014). An in vitro evaluation of novel NHA/zircon plasma coating on 316L stainless steel dental implant. *Progress in Natural Science: Materials International*, 24(2), 150-156.
- [3] Karamian, E., Abdellahi, M., Khandan, A., & Abdellah, S. (2016). Introducing the fluorine doped natural hydroxyapatite-titania nanobiocomposite ceramic. *Journal of Alloys and Compounds*, 679, 375-383.
- [4] Najafinezhad, A., Abdellahi, M., Ghayour, H., Soheily, A., Chami, A., & Khandan, A. (2017). A comparative study on the synthesis mechanism, bioactivity and mechanical properties of three silicate bioceramics. *Materials Science and Engineering: C*, 72, 259-267.
- [5] Ghayour, H., Abdellahi, M., Ozada, N., Jabbarzare, S., & Khandan, A. (2017). Hyperthermia application of zinc doped nickel ferrite nanoparticles. *Journal of Physics and Chemistry of Solids*, 111, 464-472.
- [6] Kazemi, A., Abdellahi, M., Khajeh-Sharafabadi, A., Khandan, A., & Ozada, N. (2017). Study of in vitro bioactivity and mechanical properties of diopside nano-bioceramic synthesized by a facile method using eggshell as raw material. *Materials Science and Engineering: C*, 71, 604-610.
- [7] Khandan, A., & Ozada, N. (2017). Bredigite-Magnetite ($\text{Ca}_7\text{MgSi}_4\text{O}_{16}\text{-Fe}_3\text{O}_4$) nanoparticles: A study on their magnetic properties. *Journal of Alloys and Compounds*, 726, 729-736.
- [8] Khandan, A., Jazayeri, H., Fahmy, M. D., & Razavi, M. (2017). Hydrogels: Types, structure, properties, and applications. *Biomater Tissue Eng*, 4(27), 143-69.
- [9] Sharafabadi, A. K., Abdellahi, M., Kazemi, A., Khandan, A., & Ozada, N. (2017). A novel and economical route for synthesizing akermanite ($\text{Ca}_2\text{MgSi}_2\text{O}_7$) nano-bioceramic. *Materials Science and Engineering: C*, 71, 1072-1078.
- [10] Shayan, A., Abdellahi, M., Shahmohammadian, F., Jabbarzare, S., Khandan, A., & Ghayour, H. (2017). Mechanochemically aided sintering process for the synthesis of barium ferrite: Effect of aluminum substitution on microstructure, magnetic properties and microwave absorption. *Journal of Alloys and Compounds*, 708, 538-546.
- [11] Kardan-Halvaei, M., Morovvati, M. R., & Mollaei-Darmani, B. (2020). Crystal plasticity finite element simulation and experimental investigation of the micro-upsetting process of OFHC copper. *Journal of Micromechanics and Microengineering*, 30(7), 075005.
- [12] Huang, Z.M., Zhang, Y.Z., Kotaki, M. and Ramakrishna, S., 2003. A review on polymer nanofibers by electrospinning and their applications in nanocomposites. *Composites science and technology*, 63(15), pp.2223-2253.
- [13] Feng, L., Li, S., Li, H., Zhai, J., Song, Y., Jiang, L. and Zhu, D., 2002. Super-hydrophobic surface of aligned polyacrylonitrile nanofibers. *Angewandte Chemie International Edition*, 41(7), pp.1221-1223.
- [14] Imura, K., Oi, T., Suzuki, M. and Hirota, M., 2010. Preparation of silica fibers and non-woven cloth by electrospinning. *Advanced Powder Technology*, 21(1), pp.64-68.
- [15] Li, Z. and C. Wang, 2013. Applications of Electrospun Nanofibers, in *One-Dimensional nanostructures*. Springer. p. 139-75.
- [16] Lucchini, R., Carnelli, D., Gastaldi, D., Shahgholi, M., Contro, R., & Vena, P. (2012). A damage model to simulate nanoindentation tests of lamellar bone at multiple penetration depth. In 6th European Congress on Computational Methods in Applied Sciences and Engineering, ECCOMAS 2012 (pp. 5919-5924).

- [17] Mahjoory, M., Shahgholi, M., & Karimipour, A. (2022). The effects of initial temperature and pressure on the mechanical properties of reinforced calcium phosphate cement with magnesium nanoparticles: A molecular dynamics approach. *International Communications in Heat and Mass Transfer*, 135, 106067.
- [18] Talebi, M., Abbasi-Rad, S., Malekzadeh, M., Shahgholi, M., Ardakani, A. A., Foudeh, K., & Rad, H. S. (2021). Cortical bone mechanical assessment via free water relaxometry at 3 T. *Journal of Magnetic Resonance Imaging*, 54(6), 1744-1751.
- [19] Shahgholi, M., Oliviero, S., Baino, F., Vitale-Brovarone, C., Gastaldi, D., & Vena, P. (2016). Mechanical characterization of glass-ceramic scaffolds at multiple characteristic lengths through nanoindentation. *Journal of the European Ceramic Society*, 36(9), 2403-2409.
- [20] Fada, R., Farhadi Babadi, N., Azimi, R., Karimian, M., & Shahgholi, M. (2021). Mechanical properties improvement and bone regeneration of calcium phosphate bone cement, Polymethyl methacrylate and glass ionomer. *Journal of Nanoanalysis*, 8(1), 60-79.
- [21] Razavi, M., & Khandan, A. (2017). Safety, regulatory issues, long-term biotoxicity, and the processing environment. In *Nanobiomaterials Science, Development and Evaluation* (pp. 261-279). Woodhead Publishing.
- [22] Khandan, A., Ozada, N., & Karamian, E. (2015). Novel microstructure mechanical activated nano composites for tissue engineering applications. *J Bioeng Biomed Sci*, 5(1), 1.
- [23] Ghayour, H., Abdellahi, M., Bahmanpour, M., & Khandan, A. (2016). Simulation of dielectric behavior in RFeO₃ orthoferrite ceramics (R= rare earth metals). *Journal of Computational Electronics*, 15(4), 1275-1283.
- [24] Saeedi, M., Abdellahi, M., Rahimi, A., & Khandan, A. (2016). Preparation and characterization of nanocrystalline barium ferrite ceramic. *Functional Materials Letters*, 9(05), 1650068.
- [25] Khandan, A., Karamian, E., Faghieh, M., & Bataille, A. (2014). Formation of AlN Nano Particles Precipitated in St-14 Low Carbon Steel by Micro and Nanoscopic Observations. *Journal of Iron and Steel Research International*, 21(9), 886-890.
- [26] Saeedi, M. R., Morovvati, M. R., & Mollaei-Dariani, B. (2020). Experimental and numerical investigation of impact resistance of aluminum-copper clad sheets using an energy-based damage model. *Journal of the Brazilian Society of Mechanical Sciences and Engineering*, 42(6), 1-24.
- [27] Shahverdi, S., Hajimiri, M., Esfandiari, M.A., Larijani, B., Atyabi, F., Rajabiani, A., Dehpour, A.R., Gharehaghaji, A.A. and Dinarvand, R., 2014. Fabrication and structure analysis of poly (lactide-co-glycolic acid)/silk fibroin hybrid scaffold for wound dressing applications. *International Journal of Pharmaceutics*, 473(1-2), pp.345-355.
- [28] Ghadirinejad, N., Nejad, M. G., & Alsaadi, N. (2021). A fuzzy logic model and a neuro-fuzzy system development on supercritical CO₂ regeneration of Ni/Al₂O₃ catalysts. *Journal of CO₂ Utilization*, 54, 101706.
- [29] Ghasemi, M., Nejad, M. G., & Aghaei, I. (2021). Knowledge management orientation and operational performance relationship in medical tourism (overview of the model performance in the COVID-19 pandemic and post-pandemic era). *Health Services Management Research*, 34(4), 208-222.
- [30] Ghasemi, M., Nejad, M. G., & Bagzibagli, K. (2017). Knowledge management orientation: an innovative perspective to hospital management. *Iranian journal of public health*, 46(12), 1639.
- [31] Arafat, M. T., M. M. Savalani, and I. Gibson. "Improving the mechanical properties in tissue engineered scaffolds." In *ASME 2008 International*

- Mechanical Engineering Congress and Exposition, pp. 3-6. American Society of Mechanical Engineers.
- [32] Zhang, S., 2003. Fabrication of novel biomaterials through molecular self-assembly. *Nature biotechnology*, 21(10), pp.1171-1178.
- [33] Kazemi, A., Abdellahi, M., Khajeh-Sharafabadi, A., Khandan, A., & Ozada, N. (2017). Study of in vitro bioactivity and mechanical properties of diopside nano-bioceramic synthesized by a facile method using eggshell as raw material. *Materials Science and Engineering: C*, 71, 604-610.
- [34] Morovvati, M. R., & Dariani, B. M. (2017). The effect of annealing on the formability of aluminum 1200 after accumulative roll bonding. *Journal of Manufacturing Processes*, 30, 241-254.
- [35] Rezaei, H., Asefnejad, A., Daliri-Joupari, M., & Joughehdoust, S. (2021). In-vitro cellular and in-vivo investigation of ascorbic acid and β -glycerophosphate loaded gelatin/sodium alginate injectable hydrogels for urinary incontinence treatment. *Progress in Biomaterials*, 10(2), 161-171.
- [36] Mirbebahani, F. S., Hejazi, F., Najmoddin, N., & Asefnejad, A. (2020). *Artemisia annua* L. as a promising medicinal plant for powerful wound healing applications. *Progress in Biomaterials*, 9(3), 139-151.
- [37] Baillie, L.W., 1989. The effect of sodium alginate on the antibacterial activity of chlorhexidine, gentamicin and ciprofloxacin. *The Journal of hospital infection*, 14(2), pp.171-174.
- [38] Ghahramanpoor, M.K., Najafabadi, S.A.H., Abdouss, M., Bagheri, F. and Eslaminejad, M.B., 2011. A hydrophobically-modified alginate gel system: utility in the repair of articular cartilage defects. *Journal of Materials Science: Materials in Medicine*, 22(10), pp.2365-2375.
- [39] Tonks, L., 1967. The Birth of "Plasma". *American Journal of Physics*, 35(9), pp.857-858.
- [40] Huang, D., Hu, Z.D., Ding, Y., Zhen, Z.C., Lu, B., Ji, J.H. and Wang, G.X., 2019. Seawater degradable PVA/PCL blends with water-soluble polyvinyl alcohol as degradation accelerator. *Polymer Degradation and Stability*, 163, pp.195-205.
- [41] Maghsoudlou, M. A., Barbaz Isfahani, R., Saber-Samandari, S., & Sadighi, M. (2021). The response of GFRP nanocomposites reinforced with functionalized SWCNT under low velocity impact: experimental and LS-DYNA simulation investigations. *Iranian Journal of Materials Science and Engineering*, 18(2), 0-0.
- [42] Gitiara, Y., Barbaz-Isfahani, R., Saber-Samandari, S., & Sadighi, M. (2021). Effect of nanoparticles on the improving mechanical behavior of GFRP composites in a corrosive environment. *Journal of Nanoanalysis*.
- [43] Barbaz-Isfahani, R., Saber-Samandari, S., & Salehi, M. (2022). Novel electrosprayed enhanced microcapsules with different nanoparticles containing healing agents in a single multicore microcapsule. *International Journal of Biological Macromolecules*, 200, 532-542.
- [44] Yan, E., Cao, M., Wang, Y., Hao, X., Pei, S., Gao, J., Wang, Y., Zhang, Z. and Zhang, D., 2016. Gold nanorods contained polyvinyl alcohol/chitosan nanofiber matrix for cell imaging and drug delivery. *Materials Science and Engineering: C*, 58, pp.1090-1097.
- [45] Kataria, K., Gupta, A., Rath, G., Mathur, R.B. and Dhakate, S.R., 2014. In vivo wound healing performance of drug loaded electrospun composite nanofibers transdermal patch. *International journal of pharmaceuticals*, 469(1), pp.102-110.
- [46] Karamian, E., Abdellahi, M., Khandan, A., & Abdellah, S. (2016). Introducing the fluorine doped natural hydroxyapatite-titania nanobiocomposite ceramic. *Journal of Alloys and Compounds*, 679, 375-383.
- [47] Najafinezhad, A., Abdellahi, M., Ghayour, H., Soheily, A., Chami, A., & Khandan, A. (2017). A comparative study on the synthesis mechanism, bioactivity and mechanical properties of three silicate

- bioceramics. *Materials Science and Engineering: C*, 72, 259-267.
- [48] Ghayour, H., Abdellahi, M., Ozada, N., Jabbarzare, S., & Khandan, A. (2017). Hyperthermia application of zinc doped nickel ferrite nanoparticles. *Journal of Physics and Chemistry of Solids*, 111, 464-472.
- [49] Heydari, H. A., Karamian, E., Poorazizi, E., Khandan, A., & Heydaripour, J. (2015). A novel nanofiber of Iranian gum tragacanth-polyvinyl alcohol/nanoclay composite for wound healing applications. *Procedia Materials Science*, 11, 176-182.
- [50] Karamian, E., Khandan, A., Kalantar Motamedi, M. R., & Mirmohammadi, H. (2014). Surface characteristics and bioactivity of a novel natural HA/zircon nanocomposite coated on dental implants. *BioMed research international*, 2014.
- [51] Jabbarzare, S., Abdellahi, M., Ghayour, H., Arpanahi, A., & Khandan, A. (2017). A study on the synthesis and magnetic properties of the cerium ferrite ceramic. *Journal of Alloys and Compounds*, 694, 800-807.
- [52] Karamian, E. B., Motamedi, M. R., Mirmohammadi, K., Soltani, P. A., & Khandan, A. M. (2014). Correlation between crystallographic parameters and biodegradation rate of natural hydroxyapatite in physiological solutions. *Indian J Sci Res*, 4(3), 092-9.
- [53] Khandan, A., & Esmaeili, S. (2019). Fabrication of polycaprolactone and polylactic acid shapeless scaffolds via fused deposition modelling technology. *Journal of Advanced Materials and Processing*, 7(4), 16-29.
- [54] Fazlollahi, M., Morovvati, M. R., & Mollaei Dariani, B. (2019). Theoretical, numerical and experimental investigation of hydro-mechanical deep drawing of steel/polymer/steel sandwich sheets. *Proceedings of the Institution of Mechanical Engineers, Part B: Journal of Engineering Manufacture*, 233(5), 1529-1546.
- [55] Morovvati, M. R., & Mollaei-Dariani, B. (2018). The formability investigation of CNT-reinforced aluminum nano-composite sheets manufactured by accumulative roll bonding. *The International Journal of Advanced Manufacturing Technology*, 95(9), 3523-3533.
- [56] Kjaer, I. (2013). External root resorption: Different etiologies explained from the composition of the human root-close periodontal membrane. *Dental Hypotheses*, 4(3), 75.
- [57] Motamedi, M. R. K., Behzadi, A., Khodadad, N., Zadeh, A. K., & Nilchian, F. (2014). Oral health and quality of life in children: a cross-sectional study. *Dental Hypotheses*, 5(2), 53.
- [58] Narayanan, N., & Thangavelu, L. (2015). *Salvia officinalis* in dentistry. *Dental Hypotheses*, 6(1), 27.
- [59] Khandan, A., Karamian, E., & Bonakdarchian, M. (2014). Mechanochemical synthesis evaluation of nanocrystalline bone-derived bioceramic powder using for bone tissue engineering. *Dental Hypotheses*, 5(4), 155.
- [60] Shavarani, S. M., Nejad, M. G., Rismanchian, F., & Izbirak, G. (2018). Application of hierarchical facility location problem for optimization of a drone delivery system: a case study of Amazon prime air in the city of San Francisco. *The International Journal of Advanced Manufacturing Technology*, 95(9), 3141-3153.
- [61] Mosallaeipour, S., Nejad, M. G., Shavarani, S. M., & Nazerian, R. (2018). Mobile robot scheduling for cycle time optimization in flow-shop cells, a case study. *Production Engineering*, 12(1), 83-94.
- [62] Nejad, M. G., Güden, H., & Vizvári, B. (2019). Time minimization in flexible robotic cells considering intermediate input buffers: a comparative study of three well-known problems. *International Journal of Computer Integrated Manufacturing*, 32(8), 809-819.

- [63] Ghasemi, M., Nejad, M. G., Alsaadi, N., Abdel-Jaber, M. T., Yajid, A., Shukri, M., & Habib, M. (2022). Performance measurement and lead-time reduction in epc project-based organizations: a mathematical modeling approach. *Mathematical Problems in Engineering*, 2022.
- [64] Golabi, M., & Nejad, M. G. (2022). Intelligent and fuzzy UAV transportation applications in aviation 4.0. In *Intelligent and Fuzzy Techniques in Aviation 4.0* (pp. 431-458). Springer, Cham.
- [65] Nejad, M. G., & Kashan, A. H. (2019). An effective grouping evolution strategy algorithm enhanced with heuristic methods for assembly line balancing problem. *Journal of Advanced Manufacturing Systems*, 18(03), 487-509.
- [66] Davani, P. P., Kloub, A. W. M., & Ghadiri Nejad, M. (2020). Optimizing the first type of U-shaped assembly line balancing problems. *Annals of Optimization Theory and Practice*, 3(4), 65-82.
- [67] Chehrazi, M., & Moghadas, B. K. (2022). A review on CO₂ capture with chilled ammonia and CO₂ utilization in urea plant. *Journal of CO₂ Utilization*, 61, 102030.
- [68] Denizli, A., Ali, N., Bilal, M., Khan, A., & Nguyen, T. A. (Eds.). (2022). *Nano-biosorbents for Decontamination of Water, Air, and Soil Pollution*. Elsevier.
- [69] Afrooz, M. R., Moghadas, B. K., & Tamjidi, S. (2022). Performance of functionalized bacterial as bio-adsorbent for intensifying heavy metal uptake from wastewater: A review study. *Journal of Alloys and Compounds*, 893, 162321.
- [70] Moghadas, B. K., Esmaeili, H., Tamjidi, S., & Geramifard, A. (2022). Advantages of nanoadsorbents, biosorbents, and nanobiosorbents for contaminant removal. In *Nano-Biosorbents for Decontamination of Water, Air, and Soil Pollution* (pp. 105-133). Elsevier.
- [71] Mirzapour, P., Kamyab Moghadas, B., Tamjidi, S., & Esmaeili, H. (2021). Activated carbon/bentonite/Fe₃O₄ nanocomposite for treatment of wastewater containing Reactive Red 198. *Separation Science and Technology*, 56(16), 2693-2707.
- [72] Karimianmanesh, M., Azizifard, E., Javidanbashiz, N., Latifi, M., Ghorbani, A., Shahriari, S. (2021). Feasibility study of mechanical properties of alginates for neuroscience application using finite element method. *Journal of Simulation and Analysis of Novel Technologies in Mechanical Engineering*, 13(3), 53-62.